ISSN 1087-6596, Glass Physics and Chemistry, 2017, Vol. 43, No. 5, pp. 452–458. © Pleiades Publishing, Ltd., 2017.
Original Russian Text © A.P. Solonenko, A.I. Blesman, D.A. Polonyankin, L.V. Bel'skaya, 2017, published in Fizika i Khimiya Stekla.

Peculiarities of the Composition of Solid Phases Formed in Aqueous Calcium–Silicate Systems with a Medium of Variable Acidity

A. P. Solonenko[a, *], **A. I. Blesman**[b], **D. A. Polonyankin**[b], **and L. V. Bel'skaya**[b]
[a]*Omsk State Medical University, Omsk, 644099 Russia*
[b]*Omsk State Technical University, Omsk, 644050 Russia*
**e-mail: annsolonenko@gmail.com*

Received February 14, 2017

Abstract—The effect of a medium's acidity on the composition of the solid phase formed in aqueous calcium-silicate systems is investigated. Solutions of $Ca(NO_3)_2$ and Na_2SiO_3 are used for the synthesis; the pH values were varied in the range 7.00–12.00. Freshly precipitated solid phases and products of their annealing at 1000°C were studied by the methods of Fourier IR spectroscopy, X-ray diffraction (XRD), and scanning electron microscopy (SEM).

Keywords: calcium hydrosilicates, wollastonite, precipitation of insoluble compounds from aqueous solutions, acidity of medium, silicon oxide

DOI: 10.1134/S1087659617050182

INTRODUCTION

Recently, substantial attention has been paid to fabricating synthetic analogs of calcium silicates (CSs) due to the extension of the fields of their application and their limited natural reserves. Several methods of CS synthesis are known, including the mechanochemical, sol–gel, and hydrothermal methods, as well as synthesis from solutions and suspensions [1–4]. The latter is based on the chemical precipitation of insoluble compounds in aqueous systems containing calcium ions and silicates. This method is rather simple and does not require the application of costly and/or rare reagents. For instance, calcium ions can be introduced into the reaction medium in the form of $Ca(NO_3)_2$, $CaCl_2$, $Ca(CH_3COO)_2$, or $Ca(OH)_2$, while Na_2SiO_3 is conventionally used as the source of SiO_3^{2-} ions. However, during synthesis from solutions, to ensure the satisfactory reproducibility of the composition, morphology, and dispersity of the formed solid phase, we need to thoroughly control the process parameters (reagent concentrations and ratios, temperature, pH, stirring rate, precipitate ageing conditions, etc.). For instance, on the crystallization of salts containing anions of weak polybasic acids from aqueous solutions, changes in the medium's pH could fundamentally affect the composition of the formed precipitate, since in this case a shift of the acid–base equilibrium toward the formation of other ions participating in the competitive phase-formation process is possible.

A review of the literature showed that the CS synthesis by the solution methods was performed at pH > 9 [3, 5, 6]. However, systematic studies of the effect of the pH value on the calcium-silicate phase composition have not been conducted.

The objective of this work is to study the effect of the acidity of the reaction mixture on the composition of the solid phase precipitated in aqueous solutions containing calcium salts and silicates.

EXPERIMENTAL

The interaction of aqueous solutions of $Ca(NO_3)_2$ and Na_2SiO_3 was used on the reaction

$$Ca(NO_3)_2 + Na_2SiO_3 = CaSiO_3\downarrow + 2NaNO_3. \quad (1)$$

The solutions of the initial substances of a concentration of 0.1 mol/L were prepared by the methods of weighing individual samples prior to the experiment. An equivalent volume of a Na_2SiO_3 solution was added to a solution of $Ca(NO_3)_2$ at a rate of 5 mL/min with stirring using a magnetic stirrer. Upon the mixing of the reagents, the medium's pH was corrected using HNO_3 (1 : 1) or 20% NaOH until attaining values of 7.00, 8.00, 9.00, 10.00, 11.00, or 12.00 (±0.05). The maximal pH value corresponds to the upper limit of the working range of the ES-10603/7 glass pH electrode used in combination with an I-160MI ion meter (OOO IT), whereas the minimal pH value was selected experimentally from the decrease of the degree of transformation of the Ca^{2+} ions upon precipitation (further, see Table 1). The obtained suspension

Table 1. Characteristics of crystallization of obtained solid phases

Sample	pH_{synth}	Ca/Si	$\alpha(Ca^{2+})$, %	$\alpha(SiO_3^{2-})$, %	m_{pr}, g	Δm, wt %
O12	12.00	0.97 ± 0.01	96.4 ± 0.4	99.9 ± 0.1	2.79 ± 0.08	22.9 ± 0.1
O11	11.00	0.80 ± 0.02	79.1 ± 0.3	99.4 ± 0.4	2.65 ± 0.05	21.8 ± 0.2
O10	10.00	0.60 ± 0.04	58.7 ± 0.8	97.9 ± 0.1	2.08 ± 0.06	21.0 ± 0.1
O9	9.00	0.32 ± 0.04	31.3 ± 0.7	97.4 ± 0.1	1.73 ± 0.02	18.0 ± 0.3
O8	8.00	0.10 ± 0.03	9.49 ± 0.20	97.9 ± 0.1	1.38 ± 0.11	12.4 ± 0.4
O7	7.00	0.05 ± 0.01	5.08 ± 0.45	98.0 ± 0.2	1.25 ± 0.08	11.9 ± 0.6

$\alpha(Ca^{2+})$, $\alpha(SiO_3^{2-})$ is degree of transformation of calcium and silicate ions in process of solid phase formation; m_{pr} is mass of precipitate, g; Δm is sample weight losses as result of annealing at 1000°C.

was left for 22–24 h. The formed precipitate was separated from the stock solution by filtration, washed with distilled water, dried in an air atmosphere at 90°C to a constant weight and ground in a weight mortar. Each experiment was repeated 3 times.

The products obtained through annealing the samples in air at 1000°C for 2 h were studied by the methods of X-ray diffraction analysis (XRD) using an XRD-7000 diffractometer (Shimadzu). The diffractograms' deconvolution and semiquantitative analysis were performed using a Match! software package (Crystall Impact). The IR spectra of absorption of the samples in the form of pellets with KBr were registered using an FT-801 Fourier IR spectrometer (Simex). The morphology of the solid phase particles was studied by the method of scanning electron microscopy (SEM) using a JCM-5700 electron microscope (JEOL) with a nitrogen-free energy-dispersive spectrometer for the element analysis. The precipitates were annealed in porcelain crucibles in air in a SNOL 6.7/1300 muffle furnace (SNOL-TERM).

The chemical compositions of the precipitated solid phases were found from the difference of the initial and final concentrations of the Ca^{2+} and SiO_3^{2-} ions in the stock solutions. Calcium was determined by the method of photometry in reaction with Arsenazo III in an alkaline medium; the SiO_3^{2-} ions were determined in the form of silicon-molybdenum acid in accordance with the Guidance Document (GD) 52.24.433-2005.

RESULTS AND DISCUSSION

According to the data [7], at room temperature and normal atmospheric pressure, calcium hydrosilicates (CHSs) are formed in accordance with the reaction of the ion exchange between $Ca(NO_3)_2$ and Na_2SiO_3. These are compounds of variable compositions with formula $r\mathrm{CaO} \cdot m\mathrm{SiO_2} \cdot n\mathrm{H_2O}$. The molar Ca/Si coefficient determined in [7, 8] could change in the 0.66–1.5 range. According to [8], the solid phases characterized by the value Ca/Si < 0.66 comprise mixtures of CHSs and amorphous SiO_2.

Under our experimental conditions, samples with Ca/Si ratios varying from 0.97 ± 0.01 to 0.05 ± 0.01 (Table 1) in the course of changes in the reaction medium's acidity were obtained. The stoichiometries of the precipitates formed at pH 12.00 and 11.00 are similar to those of xontolite ($Ca_6Si_6O_{17}(OH)_2$) and tobermorite ($Ca_5Si_6O_{16}(OH)_2$), respectively. The value of the Ca/Si coefficient for solid phases obtained in systems with pH 10.00 and 9.00 points to the probable formation of CHS and SiO_2 under such conditions. Here, the degree of interaction of calcium ions in the process of the precipitation of the solid phase decreases dramatically, whereas in the case of silicate ions, this parameter changes insignificantly (Table 1). The described results of the chemical analysis point to the fact that upon the acidification of the reaction medium, the CHS output decreases substantially and the Na_2SiO_3 hydrolysis resulting in formation of the amorphous silicon oxide intensifies. The latter can also explain the observed decrease of the weight of the formed solid phase (Table 1).

Changes in the composition of the samples fabricated by varying the reaction medium's acidity were corroborated by the Fourier IR spectroscopy data (Fig. 1). Along with the increase of the pH of the synthesis, the absorption maximum on the IR spectra of the solid phases shifts from 1090 to 970 cm^{-1}. According to [9], the line at 1090 cm^{-1} is attributed to the Si–O groups of silica gel ($n\mathrm{SiO_2} \cdot m\mathrm{H_2O}$), whereas the band at ~970 cm^{-1} characterizes the Si–O groups in CHS [10]. The latter is manifested on the spectrum of sample O9 in the form of a shoulder and becomes clearly discernible for the solid phases obtained in strongly alkaline media (O11, O12, Table 1). Here, the reflection at 670 cm^{-1} corresponding to the vibrations of bonds in the siloxane Si–O–Si bridges in CHS becomes clearer [10]. According to [10], the increase of the intensity of this line and its narrowing are caused by the increase of the substance's internal ordering occurring at the depolymerization of the sili-

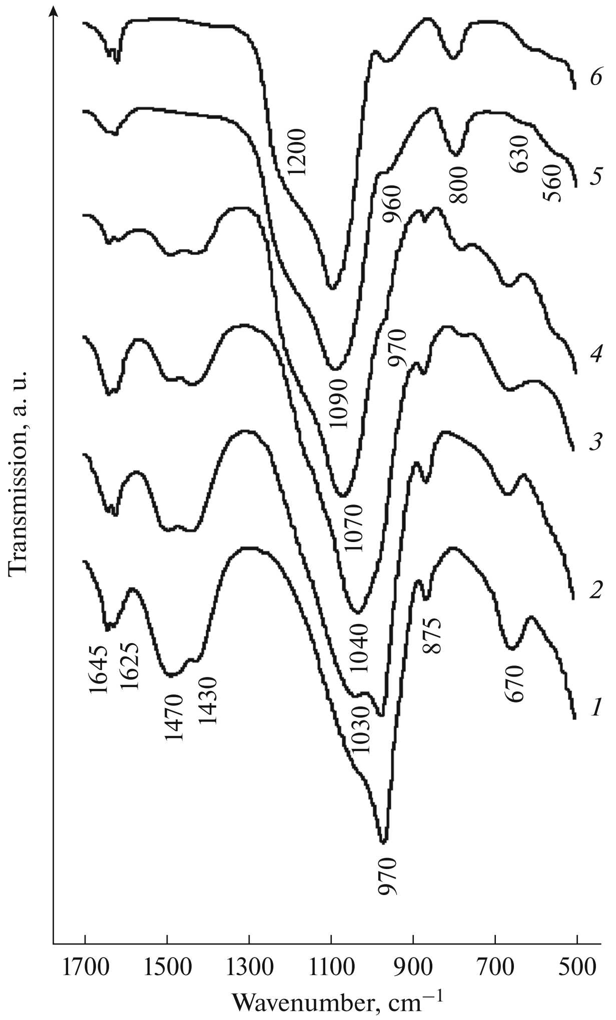

Fig. 1. IR spectra of freshly prepared samples: (*1*) O12, (*2*) O11, (*3*) O10, (*4*) O9, (*5*) O8, (*6*) O7.

cate chains due to the formation of SiO_4 silicate tetrahedra bonds with the Ca^{2+} ions. The described sample IR spectra features point to the formation of CHS in solutions with pH ≥ 9.

For samples O8 and O7 (Table 1) obtained in weakly basic and neutral solutions, only reflections characteristic of silica gel ($n\mathrm{SiO_2} \cdot m\mathrm{H_2O}$) (Fig. 1) were registered. For example, in the case of a strong band at 1090 cm^{-1} caused by the asymmetric stretching vibrations of the Si–O bonds in the composition of the amorphous SiO_2, two shoulders are discernible: at 1200 cm^{-1} (asymmetric stretching vibrations of the straightened Si–O–Si siloxane group linking the silicate chains) and 960 cm^{-1} (stretching vibrations in Si–(OH)). The intermediate-strength reflection at 800 cm^{-1} and weak bands at 630 and 560 cm^{-1} belong to the symmetric stretching vibrations of the Si–O bonds [9]. It is worth mentioning that the separate peak around 800 cm^{-1} is manifested on the spectra of samples O7–O10 and is extinguished on transition to the precipitates obtained in strongly alkaline media (Fig. 1). The latter, in combination with the transformation described above of the main maximum indicates the presence of amorphous SiO_2 in the products' composition and the decrease of its quantity in samples, along with the increase of the system's pH.

Along with the absorption bands of the groups forming the silicate framework of the precipitated phases, the IR spectra contain modes of bending vibrations of H—O—H bonds of water molecules in the capillary condensation state (1645 cm^{-1}) and dimer–monomolecular adsorbed ones (1625 cm^{-1}) [9], as well as those of the CO_3^{2-} ions (875, 1430, and 1470 cm^{-1}). The latter are discernible in the precipitate spectra for O7–O10 (Fig. 1). According to the XRD data, anions are present in the samples in the form of calcite ($CaCO_3$ of the trigonal syngony) and aragonite ($CaCO_3$ of the rhombic syngony) (Fig. 2). According to [9–11], carbonates are present in the composition of insoluble silicate compounds, since the operations of synthesis and/or ageing are carried out in open systems (in air) at an alkaline pH. Here, the formed CHSs are partially transformed into calcium carbonate (CC). Considering that the fraction of CO_3^{2-} in solutions increases along with the pH, the quantity of the formed $CaCO_3$ must, as a result, increase. The latter is corroborated by the data of Fourier transform IR spectroscopy and XRD. In the spectra of the synthesized samples, we can trace the intensification of the vibration bands of the CO_3^{2-} ions (875, 1430, and 1470 cm^{-1} [10]) at a high solution pH, while, at the same time, the intensity of the CC reflections on the diffractograms increases (Figs. 1, 2).

According to the XRD data, the crystalline form in the precipitates contains only polymorphous modifications of $CaCO_3$. Freshly precipitated CHSs and SiO_2 are weakly crystallized [9, 12], so that the widely diffused bands characterize them in the diffractograms. For example, in the case of samples O12 and O11, a low-intensity reflection in the range 2θ = 30°–35°, which can be assigned to the xontolite and tobemorite phases, is registered [4]. The presence of CHS and SiO_2 in sample O10 is responsible for the emergence of a halo in the range 2θ = 20°–35°. Upon further transition to the precipitates obtained at pH 9–7, the halo's maximum shifts to 22°. This reflection characterizes amorphous SiO_2—the main component of samples O8 and O7.

The studies of the solid phases by the SEM method demonstrated that all of the fabricated samples consisted of aggregates built from micron-size particles (Fig. 3). Their shape becomes more rounded, along with the increase of the reaction medium's acidity. The detailed examination of the SEM images of the precipitates from solutions with pH ≤ 10 allows dis-

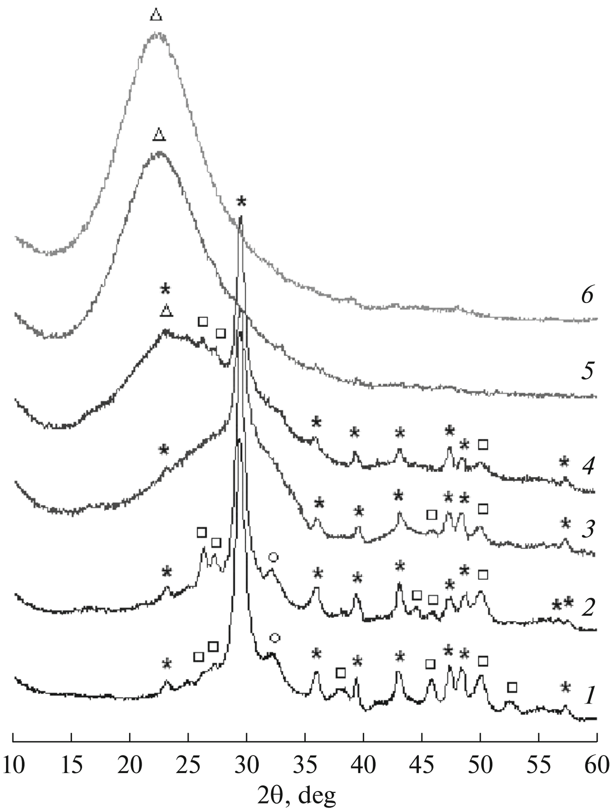

Fig. 2. Diffractograms of freshly prepared samples: (*1*) O12, (*2*) O11, (*3*) O10, (*4*) O9, (*5*) O8, (*6*) O7. * Calcite, □ aragonite, ○ CHSs, Δ silica gel.

cerning a layer of spherical SiO_2 nanogranules on the surface of the solid phase.

To sum up, the data of the chemical analysis and the results of studies of the freshly precipitated phases by the methods of Fourier IR spectroscopy, XRD, and SEM indicate the formation of CHSs of different compositions in the systems under study with pH ≥ 9. Precipitates obtained in weakly basic media (pH 9 and 10) contain, aside from $r\text{CaO} \cdot m\text{SiO}_2 \cdot n\text{H}_2\text{O}$, amorphous SiO_2. The latter becomes the main phase of the samples from solutions with pH ≤ 8.

The established features of the formation of insoluble compounds of calcium and silicon can be interpreted on examination of the ionic equilibria in solutions containing silicate anions. For instance, the Na_2SiO_3 used in this work is a salt of a weak dibasic metasilicic acid. SiO_3^{2-}, $HSiO_3^-$, and H_2SiO_3 could emerge at its dissociation in an aqueous medium. The ratio of the concentrations of these silicate forms significantly depends on the pH. As seen in Fig. 4, at a pH ≤ 8, a major part of the silicon is present in the form of H_2SiO_3 molecules. The silica gel ($n\text{SiO}_2 \cdot m\text{H}_2\text{O}$) formed upon ageing is separated from the stock solution by filtration and is studied by the methods of Fourier IR spectroscopy and XRD (Figs. 1, 2). The increase of the molar coefficient Ca/Si from the zero value for samples O7 and O8 (Table 1) must be caused by the capture of the calcium ions present in the solutions in significant quantities (0.1 mol/L) by the SiO_2 particles. Along with the increase in the pH, the larger

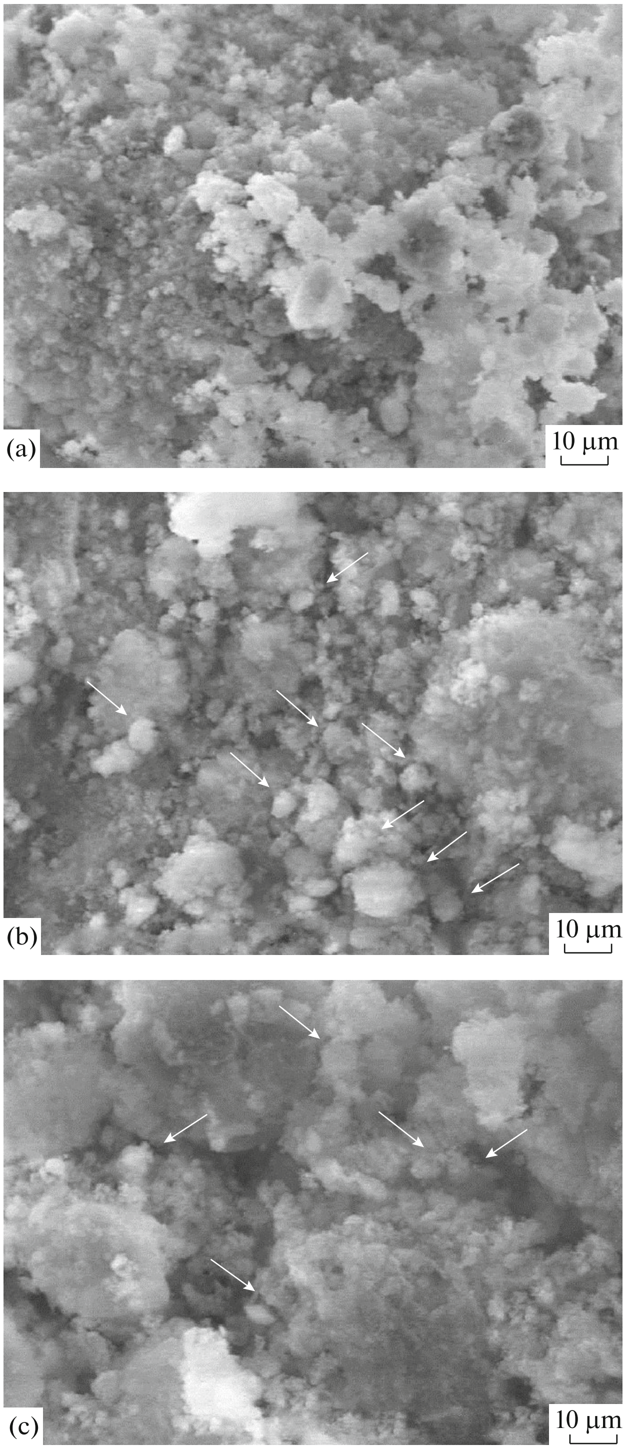

Fig. 3. SEM images of freshly prepared samples: O12 (a), O10 (b), O7 (c).

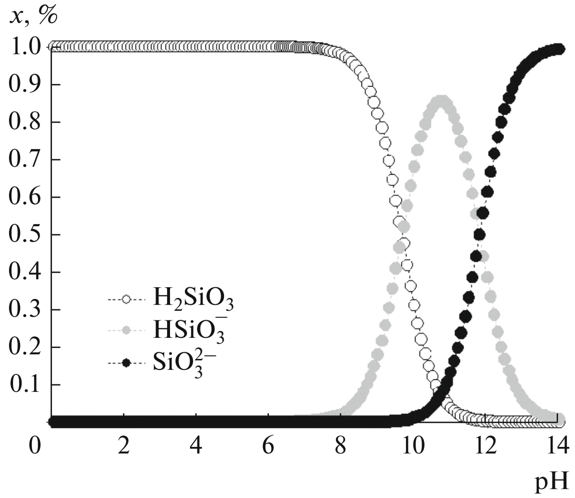

Fig. 4. Ionic diagram of metasilicic acid.

silicon fraction is transformed into anionic forms: 18% $HSiO_3^-$ + 82% H_2SiO_3 (pH 9) and 68% $HSiO_3^-$ + 31% H_2SiO_3 (pH 10). The simultaneous existence of the Ca^{2+} and $HSiO_3^-$ ions results in the formation and precipitation of the CHS phase together with amorphous silica. The reflections of CHS on the IR spectra are more intensive (and, as a result, the content in the samples is higher) the higher the pH of the stock solution and the quantity of hydrosilicates in it. In strongly alkaline media (pH ≥ 11), silicic acid is present in the systems in trace quantities, while more than 95% of the total silicon exists in the form of SiO_3^{2-} and $HSiO_3^-$. The active participation of these ions in the process of CHS formation is registered by the increase of the degree of calcium transformation (Table 1).

During annealing the samples containing amorphous phases undergo a number of transformations resulting in changes in their composition that are accompanied with mass loss (Tables 1, 2). For example, samples O7 and O8 lose ~12.5% of their total mass as a result of water removal (reaction 2). The dehydration of the precipitates is accompanied with the crystallization of the silica gel in the form of α-cristobalite. In IR spectra, it is characterized by absorption bands at 620, 790 (symmetric stretching vibrations of Si—O—Si bonds [13, 14]), 1090, and 1200 cm^{-1} (asymmetric stretching vibrations of Si—O—Si bonds [13, 14]) (Fig. 5). The diffractograms of these samples contain a peak at 2θ = 22°, corresponding to the interplane distance characteristic of α-cristobalite (4.0–4.1 Å) and a number of less intensive reflections of this phase (Fig. 6).

$$n\mathrm{SiO_2}\cdot m\mathrm{H_2O} \xrightarrow{t} \mathrm{SiO_2} + \mathrm{H_2O}\uparrow. \qquad (2)$$

β-wollastonite (β-$CaSiO_3$) is formed from the CHS-containing samples upon thermal treatment. The presence of β-$CaSiO_3$ in the annealed O9–O12 samples is registered on the absorption bands with maximums at 565, 645, 680, 902, 935, 962, 1018, 1080, and 1200 cm^{-1} on the IR spectra of the solid phases (Fig. 5). According to [15], at 565 cm^{-1}, modes of bending vibrations of the O—Si—O bonds and stretching vibrations of the Ca—O bonds in CaO_6 are manifested, the doublet in the 600–800 cm^{-1} range corresponds to the symmetric stretching vibrations of the siloxane Si—O—Si bridges, the group of peaks in the wavenumber range 850–1100 cm^{-1} is assigned to the asymmetric stretching vibrations of the Si—O bonds in SiO_4 tetrahedra, and the shoulder at 1200 cm^{-1} belongs to the asymmetric stretching vibrations of the Si—O—Si fragment linking the silicate chains in β-$CaSiO_3$. The formation of the latter was also corroborated by the XRD method (Fig. 6).

As was mentioned above, the freshly prepared O9–O12 samples contained, aside from CHSs, $CaCO_3$, which decomposes into CaO and CO_2 at 800°C [11], so that the sample loses up to 23 wt % (Table 1). The absence of calcium oxide traces in samples O9 and O10 that underwent thermal treatment can be induced by its interaction with the silica yielding the formation of β-$CaSiO_3$. However, it appears that the entire quantity of SiO_2 is not spent in this reaction, as the presence of α-cristobalite is registered in the annealed samples 09 and O10 by the methods of Fourier IR spectroscopy

Table 2. Composition of freshly prepared and annealed samples

Sample	Composition of freshly prepared samples*	Composition of samples annealed at 1000°C
O12	$Ca_6Si_6O_{17}(OH)_2$, $CaCO_3$	β-$CaSiO_3$ (94.3%), CaO (5.7%)
O11	$Ca_5Si_6O_{16}(OH)_2$, $CaCO_3$	β-$CaSiO_3$ (94%), CaO (6%)
O10	$r\mathrm{CaO}\cdot m\mathrm{SiO_2}\cdot n\mathrm{H_2O}$, $n\mathrm{SiO_2}\cdot m\mathrm{H_2O}$, $CaCO_3$	β-$CaSiO_3$ (91.2%), SiO_2 (8.8%)
O9		β-$CaSiO_3$ (84.6%), SiO_2 (15.4%)
O8	$n\mathrm{SiO_2}\cdot m\mathrm{H_2O}$	SiO_2 (100%)
O7		

* Samples' quantitative analysis was not performed due to presence of amorphous components in samples.

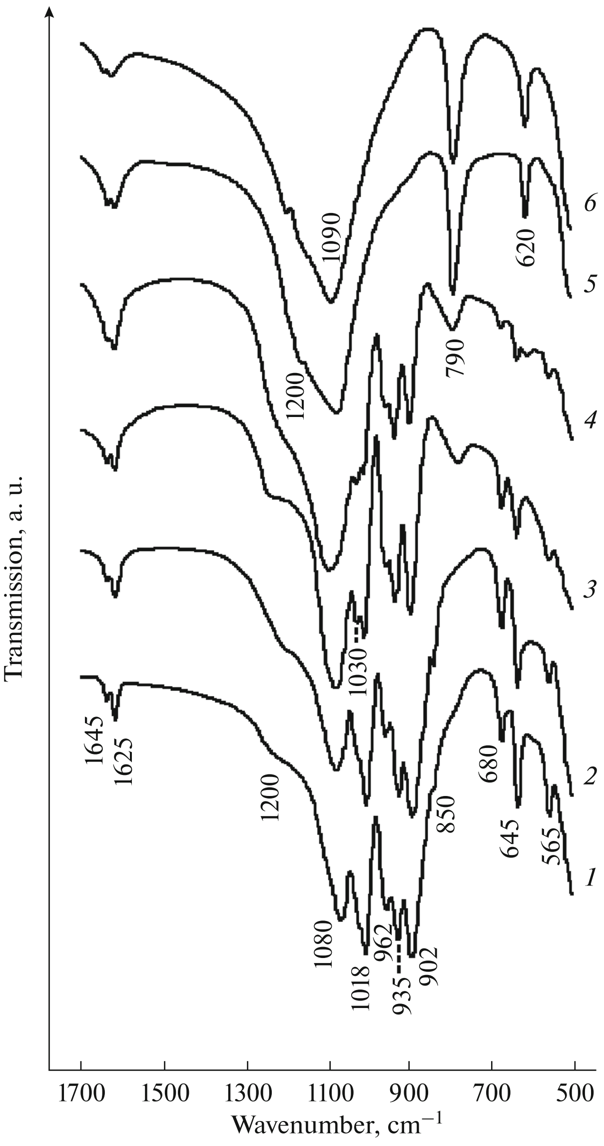

Fig. 5. IR spectra of samples annealed at 1000°C: (*1*) O7, (*2*) O8, (*3*) O9, (*4*) O10, (*5*) O11, (*6*) O12.

(the absorption bands at 620 and 790 cm^{-1}) and XRD (the reflection at $2\theta = 22°$) (Figs. 5, 6). The phase compositions of the freshly prepared and annealed samples from the data of XRD and Fourier IR spectroscopy are shown in Table 2. The data demonstrate the transformation of the initially formed phases of xontolite, tobermorite, CHSs, and silica gel into crystalline forms (β-wollastonite and α-cristobalite) occurring during two-hour annealing at 1000°C. Thus, the studies of the composition of the annealed samples corroborate the conclusions on the nature of the amorphous phases formed in calcium-silicate aqueous systems with a variable pH.

Figure 7 shows the SEM images of samples O12, O10, and O7 that underwent thermal treatment. The particles' enlargement upon annealing is clearly seen.

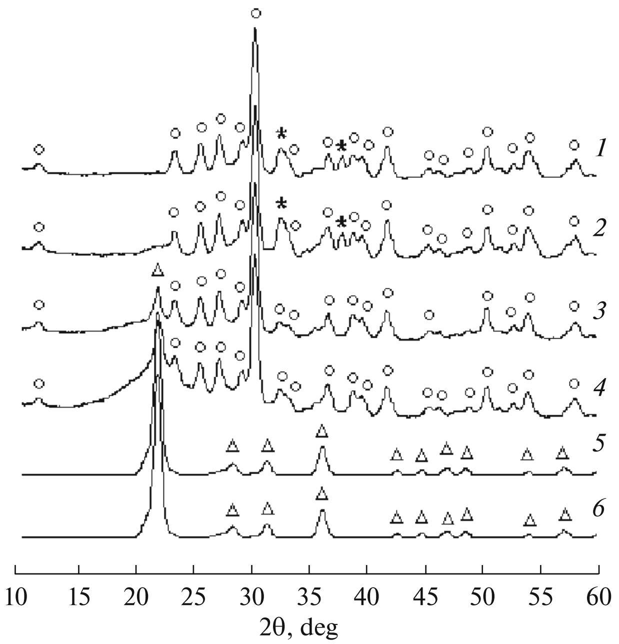

Fig. 6. Diffractograms of samples annealed at 1000°C: (*1*) O12, (*2*) O11, (*3*) O10, (*4*) O9, (*5*) O8, (*6*) O7. ○ $CaSiO_3$, Δ SiO_2, * $Ca(OH)_2$.

However, the initial heterogeneous dispersive composition of the solid phases characterized with the presence of both fine (submicron) and large (>10 μm) agglomerates is preserved.

CONCLUSIONS

A medium's acidity is an important factor determining the nature of the products formed in aqueous calcium–silicate systems. A decrease in the pH from 12.00 to 7.00 results in changes in the precipitate's composition. The data of the chemical analysis and the results of the studies by the methods of Fourier IR spectroscopy, XRD, and SEM indicate the formation of phases with the values of the Ca/Si coefficients similar to those of xontolite ($Ca_6Si_6O_{17}(OH)_2$) and tobermorite ($Ca_5Si_6O_{16}(OH)_2$) in the studied media with pH 12.00 and 11.00, respectively. At pH 10.00 and 9.00, mixtures of CHS are SiO_2 are precipitated. The samples from systems with weakly alkaline and neutral pH values consist of silica gel. The freshly prepared samples containing CHSs include an admixture of $CaCO_3$ (in the form of calcite and aragonite) formed as a result of the partial substitution of the silicate ions by the carbonate ions emerging in the reaction medium due to the dissolution of CO_2 in the air. The $CaCO_3$ decomposition and the crystallization of the amorphous components occur during the high-temperature treatment of the freshly prepared samples.

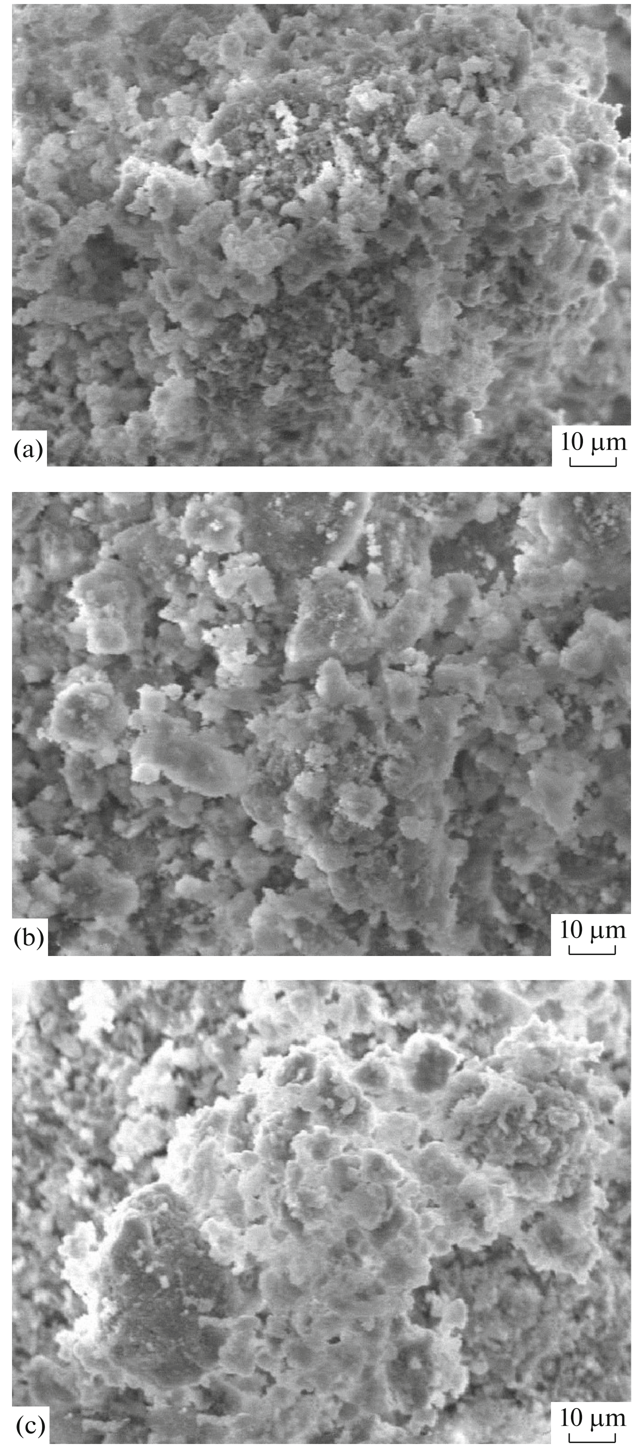

Fig. 7. SEM images of annealed samples: O12 (a), O10 (b), O7 (c).

REFERENCES

1. Meiszterics, A. and Sinko, K., Sol-gel derived calcium silicate ceramics, *Colloids Surf., A,* 2008, vol. 319, pp. 143–148.
2. Foley, E.M., Kim, J.J., and Taha, M.M.R., Synthesis and nano-mechanical characterization of calcium–silicate-hydrate (C–S–H) made with 1.5CaO/SiO$_2$ mixture, *Cement Concrete Res.,* 2012, vol. 42, pp. 1225–1232.
3. Long, L.H., Chen, L.D., and Chang, J., Low temperature fabrication and characterizations of β-CaSiO$_3$ ceramics, *Ceram. Int.,* 2006, vol. 32, pp. 457–460.
4. Akat'eva, L.V., Development of chemical technological principles of raw material treatment processes for production of calcium silicates and composition materials, *Extended Abstract of Doctoral Dissertation,* Moscow, 2014.
5. Mojumdar, S.C. and Raki, L., Preparation, thermal, spectral and microscopic studies of calcium silicate hydrate-poly(acrylic acid) nanocomposite materials, *J. Therm. Anal. Calorim.,* 2006, vol. 85, no. 1, pp. 99–105.
6. Ni, S., Lin, K., Chang, J., and Chou, L., β-CaSiO$_3$-β-Ca$_3$(PO$_4$)$_2$ composite materials for hard tissue repair: In vitro studies, *J. Biomed. Mater. Res.,* 2008, vol. 85, no. 1, p. 72.
7. Chen, J.J., Thomas, J.J., Taylor, H.F.W., and Jennings, H.M., Solubility and structure of calcium silicate hydrate, *Cement Concrete Res.,* 2004, vol. 34, p. 1499.
8. Wu, J., Zhu, Y.J., and Chen, F., Ultrathin calcium silicate hydrate nanosheets with large specific surface areas: synthesis, crystallization, layered self-assembly and applications as excellent adsorbents for drug, protein, and metal ions, *Small,* 2013, vol. 9, no. 17, pp. 2911–2925.
9. Chukin, D.G., *Khimiya poverkhnosti i stroenie dispersnogo kremnezema* (Chemistry of the Surface and Disperse Sicila Structure), Moscow: Paladin, Printa, 2008.
10. Yu, P., Kirkpatrick, R.J., Poe, B., McMillan, P.F., and Cong, X., Structure of calcium silicate hydrate (C–S–H). Near-, mid-, and far-infrared spectroscopy, *J. Am. Ceram. Soc.,* 1999, vol. 82, no. 3, pp. 742–748.
11. Yarusova, S.B., Synthesis of calcium silicates in multicomponent systems and their physicochemical properties, *Extended Abstract of Cand. Sci. Dissertation,* Vladivostok, 2010.
12. Richardson, I.G., The calcium silicate hydrate, *Cement Concrete Res.,* 2008, vol. 38, pp. 137–158.
13. Correcher, V., Garcia-Guinea, J., Bustillo, M.A., and Garcia, R., Study of the thermoluminescence emission of a natural α-cristobalite, *Radiat. Effects Defects Solids,* 2009, vol. 164, no. 1, pp. 59–67.
14. Finnie, K.S., Thompson, J.G., and Withers, R.L., Phase transitions in cristobalite and related structures studied by variable temperature infer-red emission spectroscopy, *J. Phys. Chem. Solids,* 1994, vol. 55, no. 1, pp. 23–29.
15. Luyt, A.S., Dramicanin, M.D., Antic, Z., and Djokovic, V., Morphology, mechanical and thermal properties of composites of polypropylene and nanostructured wollastonite filler, *Polym. Test.,* 2009, vol. 28, pp. 348–356.

Translated by D. Marinin